Male cuticular pheromones stimulate removal of the mating plug and promote re-mating through pC1 neurons in *Drosophila* females

Minsik Yun[1], Do-Hyoung Kim[1], Tal Soo Ha[2], Kang-Min Lee[1], Eungyu Park[1], Hany K.M. Dweck[3,5], Markus Knaden[3,4], Bill S. Hansson[3,4], Young-Joon Kim[1]*

[1]School of Life Sciences, Gwangju Institute of Science and Technology (GIST), Cheomdangwagi-ro 123, Buk-gu, Gwangju, 61005, Republic of Korea.
[2]Department of Biomedical Science, College of Natural Science, Daegu University, Gyeongsan 38453, Gyeongsangbuk-do, Korea.
[3]Department of Evolutionary Neuroethology, Max Planck Institute for Chemical Ecology, Hans-Knöll-Str. 8, 07745 Jena, Germany.
[4]Next Generation Insect Chemical Ecology, Max Planck Centre, Max Planck Institute for Chemical Ecology, Hans-Knöll-Straße 8, D-07745, Jena, Germany.
[5]Department of Entomology, The Connecticut Agricultural Experiment Station, New Haven, CT 06511, USA.

* Corresponding author: Young-Joon Kim

Email: kimyj@gist.ac.kr

Abstract

In birds and insects, females uptake sperm for a specific duration post-copulation known as the ejaculate holding period (EHP) before expelling unused sperm and the mating plug through sperm ejection. Our study uncovered that encountering males or mated females after mating substantially shortens EHP, a phenomenon we term 'male-induced EHP shortening (MIES)'. MIES requires Or47b+ olfactory and ppk23+ gustatory neurons, activated by 2-methyltetracosane and 7-Tricosene, respectively. These odorants raise cAMP levels in pC1 neurons, responsible for processing male courtship and regulating female mating receptivity. Elevated cAMP levels in pC1 neurons reduce EHP and reinstate their responsiveness to male courtship cues, promoting re-mating with faster sperm ejection. This study establishes MIES as a genetically tractable model of sexual plasticity with a conserved neural mechanism.

Significance Statement

Sexual plasticity, adapting reproductive behaviors to social changes, was explored in the fruit fly, a genetically tractable model insect. Findings revealed that inseminated females, encountering another courting male post-mating, shorten the ejaculate holding period (EHP). Specific olfactory and gustatory pathways regulating this phenomenon were identified, converging on the pC1 neurons in the brain- a conserved neural circuit regulating female mating activity. Odors associated with EHP shortening increased the second messenger cAMP. The elevated cAMP transiently heightened the excitability of pC1 neurons, enabling inseminated females to promptly remove the male ejaculate and engage in the subsequent mating more readily. This study establishes a behavioral model for sexual plasticity and provide a framework for understanding the involved neural processes.

Main Text

Introduction

Sexual plasticity, the ability to modify sexual state or reproductive behavior in response to changing social conditions, is observed in both vertebrates and invertebrates (1–5). In rodents, exposure to unfamiliar males often leads to the sudden termination of pregnancy, known as the Bruce effect. It is induced by male urinary peptides, such as MHC I peptides, activating the vomeronasal organ (6–8). This effect enhances reproductive fitness of both sexes, by eliminating the offspring of competing males and enabling females to select better mates even after conception. Many species also adapt their reproductive behaviors in response to the social sexual context change (SSCC), involving encounters with new sexual partners or

competitors. Understanding the neuronal circuit mechanisms behind female responses to SSCC emerges as a central focus in neuroscience (9–12).

Drosophila melanogaster, the fruit fly, displays various social behaviors like aggregation, aggression, and sexual behavior (13–15). Similar to rodents, they primarily use the olfactory system to communicate socially through pheromones (16, 17). Some of these pheromones act as aphrodisiacs, while others regulate aggression or foster aggregation. For instance, cis-vaccenyl acetate (cVA) attracts females but repels males and promotes aggregation (14, 18, 19). 7-Tricosene (7-T), a cuticular hydrocarbon (CHC) present in males, is an aphrodisiac to females and affects social interactions between males (20, 21). On the other hand, 7,11-Heptacosadiene (7,11-HD), a related female-specific pheromone, functions as an aphrodisiac to males, triggering courtship behavior and involving species recognition (22, 23).

The fruit fly's chemo-sensory organs, present in various body parts, detect these pheromones (24, 25). Olfactory receptor neurons (ORNs) in sensilla of the antenna and maxillary palps pick up long-range volatile pheromones like cVA, while short-range pheromones like 7-T are sensed by neurons on the fore-legs and labellum (16, 17, 24).

The olfactory receptor Or47b, expressed ORNs located in at4 trichoid sensilla on the third antennal segment, is involved in several socio-sexual interactions, including male mating success, mating partner preference, and female aggression to mating pairs (12, 26–29). In males, Or47b senses fatty acid methyl ester and fatty acid that affect mating competition and copulation (30, 31). While Or47b's role in female aggression is established (12), its involvement in female sexual behaviors is uncertain. For both sexes, the Or47b ORNs project to the VA1v glomeruli, where the VA1v projection neurons receive their signal and project to the mushroom body calyx and lateral horn. Male Or47b neurons link with neurons like aSP5, aSP8, and aSP9, which express a male-specific transcriptional factor Fru^M (32).

CHC pheromones that function as short-range pheromones are mainly detected by neurons on the fore-legs and labellum that express gustatory receptors (GR), ionotropic receptors (IR), or the ppk/DEG-ENaC family of sodium channels (16, 17, 24). CHCs like 7-T and 7,11-HD are sensed by *ppk23*-expressing M and F cells in the tarsi (33). 7-T and cVA are sensed by M cells expressing *ppk23*, while 7,11-HD and 7,11-ND are sensed by F cells expressing *ppk23*, *ppk25*, and *ppk29*. In males 7-T or 7,11-HD affects the neuronal activity of the Fru^M-expressing P1 neurons (34–36). However, how these CHCs signal in the female brain remains unknown.

Sperm ejection is a process through which females can remove the male ejaculate or the mating plug after copulation. This phenomenon was observed in various animal species including feral fowl (37), black-legged kittiwake (38), and dunnock (39). In the fruit fly, it typically occurs approximately 90 minutes after mating (40). This specific interval, referred to as ‘ejaculate holding period (EHP)’, likely affects sperm usage and fecundity (40, 41). The neurosecretory neurons in the brain pars intercerebralis (PI) that produce diuretic hormone 44 (Dh44), an insect orthologue of the corticotropin-releasing factor, regulate EHP (40). *Drosophila* females seem to signal the social sexual context through sperm ejection. For instance, when placed in the food patch with the male ejaculate deposited by other females, females exhibited increased likelihoods of egg-laying (42). However, it remains unknown whether the social sexual context influences sperm ejection and EHP.

The pC1 neurons in females, expressing a specific transcriptional factor Dsx^F, integrate olfactory and auditory cues associated with male courtship (43, 44). The female pC1 neurons in flies, their male counterparts (i.e., P1 neurons), and the ventrolateral subdivision of ventromedial hypothalamus (VMHvl) neurons in mice share conserved circuit configurations and demonstrate functional similarity in coordinating social and sexual behaviors (45, 46). There are Dsx positive 14 pC1 neurons in each brain hemisphere of the brain, responsive to the male sex-pheromone cVA and courtship songs (44, 47). Connectome analyses identified 10 pC1 neurons, categorized into five subtypes, with pC1a-c associated with mating behaviors and pC1d and e subtypes linked to aggression (47–52). Although direct evidence connecting pC1 neurons to sperm ejection is limited, they are promising candidates for regulating sperm ejection or EHP, because sperm ejection enables females to eliminate the mating plug and male ejaculate, restoring sexual attractiveness (53).

In this study, we demonstrate that two male pheromones, 2-methyltetracosane (2MC) and 7-T, significantly shorten EHP through *Or47b* neurons and *ppk23* neurons, respectively. These pheromonal pathways converge onto pC1 neurons, increasing their cAMP levels. The elevated cAMP in pC1 neurons reduced EHP, similar to the effects of the male pheromones. Elevated cAMP also enhances pC1 neuron

excitability, rendering them more responsive to both olfactory and auditory male courtship cues and promoting further mating after earlier removal of the mating plug. Our study introduces a novel behavioral paradigm, shedding light on the intricate molecular and neuronal pathways underlying female sexual plasticity.

Results

Male-induced EHP shortening (MIES) is dependent on olfaction

To investigate the impact of changes in social sexual context on EHP, we conducted a comparison between the EHP of post-mating females isolated from any male presence and those exposed to actively courting, naive wild-type *Canton-S* (*CS*) males immediately following copulation (Fig. 1A). Notably, the EHP of females incubated with naive males was approximately 30 minutes shorter than that of females left in isolation after mating (Fig. 1A, 1B). We refer to this phenomenon as 'male-induced EHP shortening (MIES)'. In contrast, there was little difference in EHP observed between females incubated with virgin females and those isolated after mating (Fig. 1C).

Male fruit flies employ various sensory signals to attract females during courtship (15). To assess the role of the visual signal in MIES, we examined MIES under dim red lighting conditions and observed that limited illumination had a marginal impact on MIES (Fig. 1D). Next, we examined MIES in post-mating females incubated with decapitated *CS* males. These males could serve as a source for olfactory or gustatory signals, but not for auditory or visual signals. Once again, we observed no reduction in MIES (Fig. 1E). This strongly suggests that olfactory or gustatory cues are the key signals responsible for MIES. This is further supported by the observation that females with a deficiency in the odorant receptor co-receptor (*Orco*^{1}) exhibited no MIES (Fig. 1F). Thus, it is highly likely that male odorant(s), especially those detected by olfactory receptors (Or), are inducing MIES.

MIES is dependent on *Or47b* receptor and *Or47b*-expressing ORNs

In fruit fly antenna, the trichoid sensilla and their associated olfactory receptor neurons are known to detect sex pheromones (54). To explore the contribution of ORNs located in the trichoid sensilla to MIES, we silenced 11 different ORN groups found in the trichoid and intermediate sensilla (55, 56) by expressing either the active or inactive form of Tetanus toxin light chain (TNT) (57). Our findings revealed that silencing ORNs expressing *Or13a*, *Or19a*, *Or23a*, *Or47b*, *Or65c*, *Or67d* or *Or88a* significantly impacted MIES (Fig. S1A).

We then focused on analyzing *Or47b*-positive ORNs (Fig. 2A), which, unlike the others, exhibited nearly complete abolition of MIES when silenced. Activation of these neurons with the thermogenetic activator dTRPA1 (58) resulted in a significant EHP shortening, even in the absence of male exposure (Fig. 2B). Subsequently, we addressed whether restoring Orco expression in *Or47b* ORNs in Orco-deficient females would restore MIES. Our results confirmed that indeed it did (Fig. 2C). To ascertain the necessity of the *Or47b* receptor gene for MIES, we examined Or47b-deficient females (*Or47b*^{2}/*Or47b*^{3}) and observed a complete absence of MIES, whereas heterozygous controls exhibited normal MIES (Fig. 2D). Furthermore, the reintroduction of *Or47b* expression in *Or47b* ORNs of *Or47b*-deficient females nearly completely restored MIES (Fig. 2E). With strength of these observations, we concluded that MIES hinges on the *Or47b* receptor gene and Or47b-expressing ORNs.

2-Methyltetracosane (2MC) induces MIES through *Or47b* and *Or47b* ORNs

Previous studies have shown that methyl laurate (ML) and palmitoleic acid (PA) can activate *Or47b* ORNs only in the presence of a functional *Or47b* gene (30, 31). However, in our investigation, none of these odorant ligands for the Or47b receptor induced significant EHP shortening, even up to 1440 ng (Fig. S2). This prompted us to seek a new pheromone capable of activating Or47b ORNs and therefore shortening EHP.

Oenocytes are known to produce a significant portion, albeit not all, of cuticular hydrocarbons or pheromones. To ascertain whether the male pheromone responsible for MIES is produced by oenocytes, we conducted experiments to determine whether incubation with females possessing masculinized oenocytes would lead to EHP shortening (Fig. S3A). Indeed, our findings confirmed that females with male oenocytes significantly shortens EHP, strongly suggesting that male oenocytes serve as a source for the MIES pheromone. Unexpectedly, however, incubation with males possessing feminized oenocytes also resulted in significant EHP shortening (Fig. S3A). This raises the possibility that oenocytes may not be the sole source of the MIES pheromone, implying the involvement of more than one pheromone, for instance one from oenocytes and another from an alternate source, in MIES.

The genus *Drosophila* exhibits distinct CHC profiles, with certain CHC components shared among closely related species (59). We found that incubation with males from other closely related species, such as *D. similans*, *D. sechellia*, and *D. erecta,* also induced EHP shortening, whereas incubation with *D. yakuba* males did not (Fig. S3B). On a search for a male-specific pheromone present in *D. melanogaster, D. similans*, *D. sechellia*, and *D. erecta*, but not in *D. yakuba* (30, 60), we identified 2MC, which shortens EHP within a physiologically relevant and narrow concentration range (Fig. 3A; Fig. S4). Moreover, EHP shortening induced by 2MC was not observed in females deficient in Orco or Or47b (Fig. 3B, 3C), but it was restored when Orco expression is reinstated in *Or47b* ORNs in Orco-deficient mutants (Fig. 3D). 2MC was found mainly in males, but not in virgin females (30). Our behavioral observations strongly indicate that 2MC acts as an odor ligand for Or47b and shortens EHP through this receptor.

7-Tricosene (7-T) shortens EHP through *ppk23* neurons

In contrast to incubation with virgin females, incubation with mated females resulted in a significant shortening in EHP (Fig. 4A). Unlike virgin females, mated females carry male pheromones, including 7-T and cVA, transferred during copulation (53). This raised the possibility that that these male pheromones might also induce EHP shortening. Indeed, our experiments revealed that incubation with a piece of filter paper infused with 150 or 375 ng of 7-T significantly shortened EHP. Conversely, incubation with cVA and 7-pentacosene, a related CHC, did not produce the same effect (Fig. 4B, 4C; Fig. S5A-5B). The concentrations of 7-T capable of inducing EHP shortening appear to be physiologically relevant. 7-T was found in quantities of 432 ng in males (61), 25 ng in virgin females, and 150 ng in mated females (53). Although the receptors for 7-T remain unknown, *ppk23*-expressing tarsal neurons have been shown to sense these compounds and regulate sexual behaviors in males and females (23, 62, 63). Subsequently, we silenced *ppk23* neurons, and as a result, MIES is almost completely abolished, underscoring the pivotal role of 7-T in MIES (Fig. 4D). However, DEG/ENac channel genes expressed in *ppk23* neurons, including *ppk23* and *ppk29*, were found to be dispensable for MIES (Fig. S5C-5E). This aligns with previous observations that neither *ppk23* deficiency nor *ppk28* deficiency replicates the sexual behavioral defects caused by silencing *ppk23* neurons (64).

A pC1 neuron subset regulates EHP and MIES

The neuropeptide Dh44 determines timing of sperm ejection or EHP (40). The same study found that Dh44 receptor neurons involved in EHP regulation also express a sexually dimorphic transcriptional factor gene *doublesex* (*dsx*). A recent study has revealed that pC1 neurons, a specific subgroup of *dsx*-expressing central neurons in the female brain, indeed express Dh44 receptors (47). With these findings, we set out to investigate the roles of pC1 neurons in the regulation of EHP and MIES. The pC1 neurons comprise five distinct subtypes. Among these, the pC1a, b, and c subtypes have been associated with mating receptivity (47, 48), while the remaining pC1d and e subtypes have been linked to female aggression (48, 52). To investigate the impact of these subtypes on EHP, we employed GtACR1, an anion channel activated by blue light in the presence of all-*trans*-retinal (ATR), to silenced specific pC1 subtypes immediately after mating. Our experiments revealed that silencing the pC1 subset comprising pC1a, b and c subtype with GtACR1 led to an increase in EHP (Fig. 5A), whereas silencing the pC1d and e subtypes had a limited effect on EHP (Fig. 5B). Furthermore, we dissected the roles of pC1b and c along with pC1a separately. We generated a subtype-specific split-Gal4 for pC1a and found that, as expected, silencing pC1a using this split-Gal4 nearly completely suppressed mating receptivity (Fig. S6). However, the silencing pC1a alone did not result in increased EHP, suggesting a marginal role of the pC1a subtype in EHP regulation (Fig. 5C). In contrast, concomitant silencing of both pC1b and pC1c significantly increased EHP by 56 $\pm$ 6.9 minutes (Fig. 5D). Currently, we lack the genetic tools required to further distinguish the roles of pC1b and pC1c subtypes individually.

Our recent research has uncovered that pC1 neurons exhibit elevated cAMP activity during sexual maturation, with this increase in cAMP being closely linked to heightened excitability of the pC1 neurons (47). The same study also revealed that a mating signal (i.e., sex peptide in the male seminal fluid) reduces cAMP activity in pC1 neurons. Thus, we hypothesized that male odorants responsible for inducing MIES, such as 2MC or 7-T, would elevate cAMP activity in pC1b and pC1c neurons in freshly mated females. This, in turn, would lead to increased excitability of pC1 neurons and, as a consequence, a reduction in the EHP. To monitor the cAMP activity in these neurons, we prepared females that selectively produce the CRE-Luciferase reporter gene in pC1b and pC1c neurons. Indeed, when exposed to 2MC or 7-T, pC1b and pC1c neurons exhibited a significant increase in CRE-luciferase activity, indicating that these neurons produce higher levels of cAMP in response to these odorants (Fig. 5E). Notably, the CRE-Luciferase activity appeared to reach its peak at specific odorant concentrations that induced a significant shortening of EHP (Fig. S7).

In contrast, when examining other pC1 subsets, such as pC1a, and pC1d and e, we detected no sign of increased CRE-Luciferase reporter activity upon exposure to 2MC or 7-T treatment (Fig. 5E). It is worth noting that CRE-luciferase reporter activity in the pC1a neurons appears to be dependent on the mating status, as it reaches levels similar to those of pC1b and pC1c neurons in virgin females (Fig. S8). This observation aligns well with connectome data, which indicates that SAG neurons, responsible for relaying SP-dependent mating signals, primarily establishes synapses into pC1a subtype and to a much lesser extent into other pC1 subtypes (49).

Having shown that MIES-inducing male odorants, 2MC or 7-T, increase cAMP activity in pC1b and pC1c neurons from mated females, we next asked whether this induced elevation of cAMP levels in pC1b and pC1c would shorten EHP, leading to MIES. We employed the photoactivatable adenylate cyclase (PhotoAC), which augments cellular cAMP levels upon exposure to light. Indeed, the induced elevation of cAMP activity in pC1b and pC1c significantly shortened EHP, whereas the same treatment applied to pC1a or pC1d and pC1e had no such effect (Fig. 5F). This further underscores the pivotal role of pC1b and pC1c in EHP regulation.

Next, we asked whether the expression of Dh44R1 and Dh44R2, GPCRs that increase cellular cAMP in response to their ligand Dh44, in pC1b and pC1c neurons is necessary for MIES. However, double knockdown of Dh44R1 and Dh44R2 in pC1 neurons seemed to have a limited impact on MIES (Fig. S9). This suggests that Dh44R signaling in pC1 neurons is not essential for the regulation of EHP or MIES, opening up the possibility that other GPCRs may be involved in up-regulating cAMP levels in pC1 neurons in response to 2MC or 7-T.

Lastly, we investigated how the increased cAMP activity affects physiological activity of pC1 neurons. pC1 neurons from virgin females exhibit robust Ca^{2+} transients in response to male courtship cues, such as the male pheromone cVA and courtship pulse song (44). In contrast, those from mated females display significantly diminished Ca^{2+} transients (47). Shortly after mating, a decrease in pC1 responsiveness to cVA was observed. However, immediately following the activation of PhotoAC in pC1 neurons, pC1 neurons in freshly mated females became more excitable and exhibited stronger Ca^{2+} transients in response to cVA (Fig. 5G). It is important to note that this PhotoAC-induced increase in pC1 excitability is transient and diminishes rapidly within 10 minutes (Fig. 5G). Together, these findings suggest that the increased cAMP levels in pC1 neurons would not only promote MIES but also facilitate re-mating in post-mating females, which typically engage in additional mating at a low frequency. To test this hypothesis, we examined the re-mating frequency of freshly mated females paired with naive males while inducing a cAMP increase in pC1 neurons. As expected, PhotoAC activation in pC1b and c neurons substantially increased the re-mating rate compared to the control group (Fig. 5H). Therefore, we concluded that male odorants, which stimulate cAMP elevation in pC1 neurons. expedite the removal of mating plug, consequently leading to increased instances of re-mating.

Discussion

Males employ a diverse range of strategies to enhance their reproductive fitness. One such strategy involves the formation of a 'mating plug', a mechanism that prevents females from engaging in further mating and consequently increases fertilization success rates (65–67). As a means of intra-sexual competition, rival males often promote the removal or precocious expulsion of the mating plug. This behavior is driven by the fact that polyandrous females often eliminate the mating plug to engage in additional mating with males possessing superior traits or higher social status than their previous partners (37, 68). In the dunnock (*Prunella modularis*), a small European passerine bird, the male often engages in cloacal pecking of copulated females, inducing the expulsion of prior mate's sperm and mating plug, thereby increasing their chance of successful mating (39). In this study, we discovered that in *D. melanogaster*, when kept with actively courting males, freshly mated females exhibit an earlier removal of the mating plugs or a shorter EHP. This behavior is primarily induced by the stimulation of females via male sex pheromones. Furthermore, our study has uncovered the conserved neural circuitry that processes male courtship cues and governs mating decisions play an important role in regulating this behavior. By delving into the molecular and neuronal mechanisms underlying MIES, our study provides valuable insights into the broader aspect of behaviors induced by social sexual context changes.

Our findings highlight the involvement of the Or47b receptor and Or47b ORNs in MIES. These OR and ORNs have been linked to a range of social and sexual behaviors in both males and female fruit flies (12, 26–31). Methyl laurate and trans-palmitoleic acid are odor ligands for Or47b, which explain many of these functions particularly in males (30, 31). In this study, we provide compelling evidence that 2MC induces EHP shortening via both Or47b receptor and Or47b ORNs, suggesting that 2MC functions as an odor

ligand for Or47b. Notably, a gas chromatography–mass spectrometry (GC-MS) analysis of cuticular hydrocarbons of 4-day-old wild type *D. melanogaster* indicated the presence of 2MC solely in males, excluding females (30). Surprisingly, however, unlike 2MC, neither methyl laurate nor trans-palmitoleic acid influences EHP. The reason of this paradoxical results remains unclear. Plausible interpretation is that the EHP shortening induced by 2MC may require not only Or47b but also other as-yet-unidentified ORs. With the establishment of a behavioral and cellular assessment for 2MC activity, the search for additional odorant receptors responsive to 2MC is now feasible. An other important avenue for further research is whether 2MC can also elicit behaviors that were previously associated with methyl laurate or trans-palmitoleic acid, such as the promotion of male copulation and courtship (30, 31).

We observed that both 2MC and 7-T exhibit both cellular and behavioral activity within a specific concentration range (Fig. S4, S5, S7). This observation is of particularly interest, given the multitude of environmental and biological factors that influence the levels of 2MC and 7-T, potentially affecting the capacity of males to induce MIES. For instance, exposure to low temperatures during development has been linked to increased production of both 2MC and 7-T (69). Similarly, the mutation of the desiccation stress gene CG9186, which encodes a protein associated with lipid droplet, has been found to impact 2MC levels (70). Furthermore, 2MC levels rise with the aging of males (71). Thus, we propose that the levels of 2MC and possibly 7-T may serve as indicators of male's age and their resilience against environmental stresses in a complex and non-linear manner.

In mated females, treatment with 2MC or 7-T increases cAMP activity in pC1b,c neurons but not in pC1a neurons. In contrast, pC1a neurons in virgin females are fully responsive to both male pheromones, showing a cAMP activity that is similar to that of pC1b,c neurons (Fig. S8). The absence of cAMP activity in pC1a neurons in mated females likely results from the mating signal (i.e., sex peptide) silencing pC1a neurons. Connectome and electrophysiology data support this interpretation, as SAG neurons, which relay sex peptide signals, exhibit the strongest synaptic connection with pC1a subtype among five pC1 subtypes (49). However, SAG neuron activity may also influence pC1c neurons, as they also have substantial synaptic connections with pC1c neurons in hemibrain (72). Notably, induced activation of SAG neurons significantly shortens EHP (Fig. S10), suggesting they regulate EHP through pC1c neurons.

We found that increased cAMP levels causes pC1b,c neurons in mated females, which typically do not respond to male courtship cues like cVA and pulse song, to become responsive, showing strong Ca^{2+} transients. Since pC1b,c neurons play a role in generating sexual drive and increasing female receptivity to male courtship, the 2MC or 7-T-induced increases in cAMP likely govern the removement of the mating plug and engagement in further mating of mated females. This observation well aligns with the previous report that mating reduces sensitivity of Or47b ORNs, which we find responsive to 2MC, leading to the increased preference for pheromone-rich males after mating (29). Moreover, the finding that 2MC and 7-T induce cAMP activity in pC1b,c neurons in virgin females suggests that virgin females may also use 2MC and 7-T as odorant cues to assess male quality during their first mating. Indeed, females seem to evaluate male quality with the amount of 7-T, as increased 7-T promotes mating receptivity and shortens mating latency (20).

Physiological factors like the nutritional status of females before mating and the nutritional status of their mating partners have been shown to influence EHP (73), and therefore potentially MIES. Hence, it is highly probable that MIES is regulated by additional central neurons such as Dh44-PI neurons that regulate these processes (40). However, it remains unclear whether and how Dh44-PI neurons and pC1 neurons interact to modulate EHP and MIES. The observation that double knockdown of Dh44R1 and Dh44R2 has only a marginal effect on MIES suggests that Dh44-PI neurons may also function independently of pC1 neurons, suggesting the possibility that multiple independent central circuits may contribute to the production of MIES.

Our initial screening of ORNs responsible for MIES revealed the involvement of Or47b ORNs, as well as several other ORNs. In addition to 2MC, which operates through Or47b expressing ORNs, our findings indicate that 7-T and *ppk23* neurons capable of detecting 7-T also play a role in MIES induction. In *D. melanogaster* and other related species, food odors typically serve as long-range signals that attract both males and females (74, 75), implying that certain food odors might also influence EHP (42). The involvement of multiple odorants and ORNs in EHP regulation implicates that pC1 neurons can process various cues, not restricted to those associated with mating behaviors, including food odors. Future studies will explore the full spectrum of odorants processed by pC1 neurons in EHP regulation.

In conclusion we have identified a circuit that, via the detection of a novel male pheromone, potentially signals male quality and governs the female decision to remove the mating plug of its last mate and mate again.

Materials and Methods

Fly care

Flies were cultured on a standard medium composed of dextrose, cornmeal, and yeast, under room temperature in a 12hr : 12hr light:dark cycle (40, 73). Behavioral assays were performed at 25 °C, except for thermal activation experiment with dTRPA1. Virgin males and females were collected immediately after eclosion. Males were individually aged for 4-6 days, while females were aged in groups of 15–20. For EHP and mating assays, females were aged for 3-4 days. Assays were performed at Zeitgeber time (ZT) 3:00–11:00, and were repeated at least on three separate days.

Fly stocks

The following stocks are from the Bloomington *Drosophila* Stock Center (BDSC), the Vienna *Drosophila* Resource Center (VDRC): *Canton S (CS)* (RRID: BDSC_64349), w^{1118} (VDRC #60000), *R71G01* (pC1-Gal4) (RRID: BDSC_39599), *Orco1* (RRID: BDSC_23129), *Or13a-Gal4* (RRID: BDSC_9946), *Or19a-Gal4* (RRID: BDSC_9948), *Or23a-Gal4* (RRID: BDSC_9955), *Or43a-Gal4* (RRID: BDSC_9974), *Or47b-Gal4* (RRID: BDSC_9983), *Or47b-Gal4* (RRID: BDSC_9984), *Or65a-Gal4* (RRID: BDSC_9993), *Or65b-Gal4* (RRID: BDSC_23901), *Or65c-Gal4* (RRID: BDSC_23903), *Or67d-Gal4* (RRID: BDSC_9998), *Or83c-Gal4* (RRID: BDSC_23131), *Or88a-Gal4* (RRID: BDSC_23137), *UAS-Or47b* (RRID: BDSC_76045), *Or47b2/2* (RRID: BDSC_51306), *Or47b3/3* (RRID: BDSC_51307), *UAS-TNT active* (RRID: BDSC_28837), *UAS-TNT inactive* (RRID: BDSC_28839), *UAS-dTRPA1* (RRID: BDSC_26263), *UAS-CsChrimson* (RRID: BDSC_55135), *UAS-GCaMP6m* (RRID: BDSC_42748), *R52G04-AD* (RRID: BDSC_71085), *SAG-Gal4* (VT50405) (RRID:Flybase_FBst0489354, VDRC #200652), *UAS-Dh44R1-RNAi* (RRID:Flybase_FBst0482273, VDRC #110708), *UAS-Dh44R2-RNAi* (RRID:Flybase_FBst0465025, VDRC #43314), *UAS-Dicer2* (VDRC #60007). The following stocks are reported previously: *PromE(800)-Gal4* (59), *UAS-FLP, CRE-F-luc* (76), *LexAop-FLP* (77), *UAS-CsChrimson* (78), *UAS-GtACR1* (79), *UAS-PhotoAC* (PACα) (80), pC1-A (48), pC1-S (48), *Dh44-pC1-Gal4* (47), *ppk23-Gal4*, *ppk23-*, *ppk28-*, *ppk29-* (62), and *Orco-Gal4*, *UAS-EGFP-Orco* (81). *pC1a-split-Gal4* is generated by combining *R52G04-AD* (RRID: BDSC_71085) and *dsx-DBD* (49). *Drosophila* subgroups species are obtained from the EHIME-Fly *Drosophila* stock center. To enhance knock-down efficiency, RNAi experiments were performed using flies carrying *UAS-Dicer2* (VDRC #60007).

Chemical information

All trans-retinal (Cat# R2500), methyl laurate (Cat# W271500), and Triton™ X-100 (Cat# X100) were obtained from Sigma-Aldrich (St. Louis, MO, USA). The following chemicals are from the Cayman chemical (Ann Arbor, MI, USA): 7(Z)-Tricosene (CAS No. 52078-42-9, Cat# 9000313), 7(Z)-Pentacosene (CAS No. 63623-49-4, Cat# 9000530), *trans*-palmitoleic acid (CAS No. 10030-73-6, Cat# 9001798), 11-*cis*-vaccenyl acetate (cVA) dissolved in EtOH (CAS No. 6186-98-7, Cat# 10010101). 2-methyltetracosane (>98%, purity) was custom-synthesized by KIP (Daejeon, Korea).

Behavior assays

For mating behavior assays, we followed the procedures described previously (82). Individual virgin females and naive *CS* males were paired in chambers with a diameter of 10 mm and were recorded using a digital camcorder (SONY, HDR-CX405 or Xiaomi, Redmi Note 10) for either 30 min or 1 hour for the mating assay and 6 hours for the re-mating assay. In the re-mating assay, females that completed their initial mating within 30 min were subsequently paired with naive *CS* males.

To measure EHP, which is defined as the time elapsed between the end of copulation and sperm ejection, we used the following procedure: Virgin females were paired individually with *CS* males in 10-mm diameter chambers. Following copulation, females were transferred to new chambers, either with or without a *CS* male or a piece of filter paper treated with pheromones, and their behavior was recorded using a digital camcorder (SONY, HDR-CX405). Typically, females that completed copulation within 30 minutes were used for analysis. To present the pheromone, females were individually kept in 10-mm diameter chambers containing a piece of Whatman filter paper (2 mm x 2 mm) that had been treated with 0.5 μl of the pheromone solution and left to air dry for 1 minute. For thermal activation experiments, females were incubated at the specified temperatures immediately after copulation ended. For light-activation experiments, a custom-made light activation setup utilizing a ring of 104 multi-channel LED lights (NeoPixel, Cat# WS2812; Red light, 620-625 nm, 390-420 mcd; Green light, 522-525 nm, 660-720 mcd;

Blue light, 465-467 nm, 180-200 mcd) was employed. Females were individually placed in 10-mm diameter chambers, and the chamber was illuminated with light at an intensity of 1100 lux across the chamber, as measured by a lightmeter HS1010, during the assay. Flies used in these experiments were prepared by culturing them in food containing vehicle (EtOH) or 1 mM all-trans-retinal (ATR) immediately after eclosion. They were kept in complete darkness for 3-4 days until the assay was conducted.

Calcium imaging

We followed the procedures described previously (47, 83). Following copulation, freshly mated female fly was temporally immobilized using ice anesthesia, and its head was attached to a custom made thin metal plate with a 1mm diameter hole using photo-curable UV glue (ThreeBond, A16A01). An opening in the fly's head was generated using a syringe needle under saline (108 mM NaCl, 5 mM KCl, 2 mM $CaCl_2$, 8.2 mM $MgCl_2$, 4 mM $NaHCO_3$, 1 mM NaH_2PO_4, 5 mM trehalose, 10 mM sucrose, 5 mM HEPES pH 7.5). Imaging was performed using Zeiss Axio Examiner A1 microscope equipped with an electron multiplying CCD camera (Andor Technology, Luca^{EM} R 604M) and a LED light-source (CoolLED, Precis Excite). Imaging analysis was used Metamorph software (Molecular Devices, RRID:SCR_002368). To deliver the male pheromone using an airflow, we used the Syntech Stimulus Controller (Type CS-55). 2 μl of pheromone solution was applied to a piece of Whatman filter paper (2 mm x 1 mm), which was then inserted into a glass Pasteur pipette after solvent evaporation.

Luciferase assay

We followed the procedures described previously (47, 76). 3-day-old virgin females or freshly mated females were used for assay. A group of three fly heads, kept at -80°C, was homogenized using cold homogenization buffer (15 mM HEPES, 10 mM KCl, 5 mM $MgCl_2$, 0.1 mM EDTA, 0.5 mM EGTA). Luciferase activity was measured by using beetle Luciferin, potassium Salt (Promega, Cat# E1603) and a microplate Luminometer (Berthold technologies, Centro XS^3 LB 960), following manufacturer's instructions. To present the odorant, flies were placed in 10-mm diameter chambers containing a piece of Whatman filter paper (4 mm x 6 mm) that had been treated with 1 μl of the pheromone solution and left to air dry for 1 minute.

Immunohistochemistry

3–5-day-old virgin female flies were dissected in phosphate-buffered saline (PBS) and fixed for 30 minutes at room temperature in 4% paraformaldehyde in PBS. Following fixation, the brains were thoroughly washed in PBST (0.1% Triton™ X-100 in PBS) and then blocked using 5% normal goat serum in PBST. After blocking, the brains were incubated with the primary antibody in PBST for 48 hours at 4 °C, washed by PBST and then incubated with the secondary antibody in PBST for 24 hours at 4 °C. The samples were washed three times with PBST and once with PBS before being mounted in Vectashield (Vector Laboratories, Cat# H-1000). Antibodies used were rabbit anti-GFP (1:1000; Thermo Fisher Scientific, Cat# A-11122, RRID:AB_221569), mouse anti-nc82 (1:50; Developmental Studies Hybridoma Bank, Cat# Nc82; RRID: AB_2314866), Alexa 488-conjugated goat anti-rabbit (1:1000; Thermo Fisher Scientific, Cat# A-11008, RRID:AB_143165), Alexa 568-conjugated goat anti-mouse (1:1000; Thermo Fisher Scientific, Cat# A-11004, RRID:AB_2534072). Brain images were acquired using Zeiss LSM 700/Axiovert 200M (Zeiss) and processed using Fiji (https://imagej.net/software/fiji/downloads, RRID:SCR_002285)

Color-depth MIP based anatomy analysis

A stack of confocal images from *pC1a-split-Gal4>UAS-myr-EGFP* adult female brains stained with anti-GFP and anti-nc82 were used. Images were registered onto the JRC2018 unisex brain template (84). using the Computational Morphometry Toolkit (CMTK, https://github.com/jefferis/fiji-cmtk-gui). Color depth MIP masks of *pC1a-split-Gal4* neurons and pC1a (ID, 5813046951) in Hemibrain (72) (Fig. S6A) were generated using the ColorMIP_Mask_Search plugin (85) for Fiji (https://github.com/JaneliaSciComp/ColorMIP_Mask_Search) and NeuronBridge (86) (https://neuronbridge.janelia.org/). Similarity score and rank were calculated using NeuronBridge.

Statistical analysis

Statistical analysis was conducted using GraphPad Prism 9 (Graphpad, RRID:SCR_002798), with specific details on each statistical method provided in the figure legends.

Acknowledgments

We thank S. Kang, J-H. Yoon, B. Lee for excellent technical assistance. Fly stocks were obtained from the Bloomington *Drosophila* Stock Center (NIH P40OD018537), the Vienna *Drosophila* Resource Center (VDRC), the Kyoto Stock Center, EHIME-Fly *Drosophila* species stock center, KYORIN-Fly *Drosophila*

species stock center, and the Korea *Drosophila* Resource Center (NRF-2022M3H9A1085169). This work was supported by National Research Foundation of Korea grants NRF-2022R1A2C3008091 (Y-J.K.), 2022M3E5E8081194 (Y-J.K.), NRF-2019R1A4A1029724 (Y-J.K.), GIST Research Institute (GRI) GIST-MIT research collaboration grant funded by the GIST in 2022 (Y-J.K.), 2023 GIST grant (Y-J.K.), 2017R1A6A3A11027866 (D-H.K.), NRF-2021R1I1A1A01060304 (D-H.K.), 2022 AI-based GIST Research Scientist Project (D-H.K.) and 2023 AI-based GIST Research Scientist Project (D-H.K.).

Author contributions: Conceptualization: M.Y., Y-J.K., Methodology: K-M.L., H.K.M.D., M.K., B.S.H., Investigation: M.Y., D-H.K., T.S.H., E.P., Visualization: M.Y., Supervision: Y-J.K., Writing—original draft: M.Y., Y-J.K., Writing—review & editing: M.Y., M.K., B.S.H., Y-J.K.

Competing interests: The authors declare that they have no competing interest.

Keywords: sexual plasticity; sperm ejection; pC1; Or47b; ppk23

References

1. B. Yagound, P. Blacher, S. Chameron, N. Châline, Social context and reproductive potential affect worker reproductive decisions in a eusocial insect. *PLoS One* **7**, e52217 (2012).

2. H. M. Bruce, An exteroceptive block to pregnancy in the mouse. *Nature* **184**, 105 (1959).

3. E. K. Roberts, A. Lu, T. J. Bergman, J. C. Beehner, A Bruce effect in wild geladas. *Science* **335**, 1222–1225 (2012).

4. S. Steiger, R. Franz, A.-K. Eggert, J. K. Müller, The Coolidge effect, individual recognition and selection for distinctive cuticular signatures in a burying beetle. *Proc Biol Sci* **275**, 1831–1838 (2008).

5. J. M. Koene, A. Ter Maat, Coolidge effect in pond snails: male motivation in a simultaneous hermaphrodite. *BMC Evol Biol* **7**, 212 (2007).

6. T. Leinders-Zufall, *et al.*, MHC class I peptides as chemosensory signals in the vomeronasal organ. *Science* **306**, 1033–1037 (2004).

7. S. D. Becker, J. L. Hurst, Pregnancy Block from a Female Perspective in *Chemical Signals in Vertebrates 11*, J. L. Hurst, R. J. Beynon, S. C. Roberts, T. D. Wyatt, Eds. (Springer, 2008), pp. 141–150.

8. M. N. Zipple, E. K. Roberts, S. C. Alberts, J. C. Beehner, Male-mediated prenatal loss: Functions and mechanisms. *Evol Anthropol* **28**, 114–125 (2019).

9. D.-W. Kim, *et al.*, Multimodal Analysis of Cell Types in a Hypothalamic Node Controlling Social Behavior. *Cell* **179**, 713-728.e17 (2019).

10. D. Wei, V. Talwar, D. Lin, Neural circuits of social behaviors: Innate yet flexible. *Neuron* **109**, 1600–1620 (2021).

11. M. Liu, D.-W. Kim, H. Zeng, D. J. Anderson, Make war not love: The neural substrate underlying a state-dependent switch in female social behavior. *Neuron* **110**, 841-856.e6 (2022).

12. M. Gaspar, S. Dias, M. L. Vasconcelos, Mating pair drives aggressive behavior in female Drosophila. *Curr Biol* **32**, 4734-4742.e4 (2022).

13. R. J. Bartelt, A. M. Schaner, L. L. Jackson, cis-Vaccenyl acetate as an aggregation pheromone inDrosophila melanogaster. *J Chem Ecol* **11**, 1747–1756 (1985).

14. J.-C. Billeter, J. Levine, The role of cVA and the Odorant binding protein Lush in social and sexual behavior in Drosophila melanogaster. *Frontiers in Ecology and Evolution* **3** (2015).

15. J.-C. Billeter, E. J. Rideout, A. J. Dornan, S. F. Goodwin, Control of male sexual behavior in Drosophila by the sex determination pathway. *Curr Biol* **16**, R766-776 (2006).

16. S. Sengupta, D. P. Smith, "How Drosophila Detect Volatile Pheromones: Signaling, Circuits, and Behavior" in *Neurobiology of Chemical Communication*, Frontiers in Neuroscience., C. Mucignat-Caretta, Ed. (CRC Press/Taylor & Francis, 2014) (October 18, 2023).

17. J. Kohl, P. Huoviala, G. S. Jefferis, Pheromone processing in Drosophila. *Curr Opin Neurobiol* **34**, 149–157 (2015).

18. A. Kurtovic, A. Widmer, B. J. Dickson, A single class of olfactory neurons mediates behavioural responses to a Drosophila sex pheromone. *Nature* **446**, 542–546 (2007).

19. S. D. Mane, L. Tompkins, R. C. Richmond, Male Esterase 6 Catalyzes the Synthesis of a Sex Pheromone in Drosophila melanogaster Females. *Science* **222**, 419–421 (1983).

20. M. Grillet, L. Dartevelle, J.-F. Ferveur, A Drosophila male pheromone affects female sexual receptivity. *Proc Biol Sci* **273**, 315–323 (2006).

21. L. Wang, *et al.*, Hierarchical chemosensory regulation of male-male social interactions in Drosophila. *Nat Neurosci* **14**, 757–762 (2011).

22. C. Antony, T. L. Davis, D. A. Carlson, J. M. Pechine, J. M. Jallon, Compared behavioral responses of maleDrosophila melanogaster (Canton S) to natural and synthetic aphrodisiacs. *J Chem Ecol* **11**, 1617–1629 (1985).

23. H. Toda, X. Zhao, B. J. Dickson, The Drosophila female aphrodisiac pheromone activates ppk23(+) sensory neurons to elicit male courtship behavior. *Cell Rep* **1**, 599–607 (2012).

24. R. M. Joseph, J. R. Carlson, Drosophila Chemoreceptors: A Molecular Interface Between the Chemical World and the Brain. *Trends Genet* **31**, 683–695 (2015).

25. M. Z. Ali, null Anushree, A. L. Bilgrami, J. Ahsan, Drosophila melanogaster Chemosensory Pathways as Potential Targets to Curb the Insect Menace. *Insects* **13**, 142 (2022).

26. S. R. Lone, A. Venkataraman, M. Srivastava, S. Potdar, V. K. Sharma, Or47b-neurons promote male-mating success in Drosophila. *Biol Lett* **11**, 20150292 (2015).

27. S. R. Lone, V. K. Sharma, Or47b receptor neurons mediate sociosexual interactions in the fruit fly Drosophila melanogaster. *J Biol Rhythms* **27**, 107–116 (2012).

28. L. Zhuang, *et al.*, Or47b plays a role in Drosophila males' preference for younger mates. *Open Biol* **6**, 160086 (2016).

29. P. Kohlmeier, Y. Zhang, J. A. Gorter, C.-Y. Su, J.-C. Billeter, Mating increases Drosophila melanogaster females' choosiness by reducing olfactory sensitivity to a male pheromone. *Nat Ecol Evol* **5**, 1165–1173 (2021).

30. H. K. M. Dweck, *et al.*, Pheromones mediating copulation and attraction in Drosophila. *Proc Natl Acad Sci U S A* **112**, E2829-2835 (2015).

31. H.-H. Lin, *et al.*, Hormonal Modulation of Pheromone Detection Enhances Male Courtship Success. *Neuron* **90**, 1272–1285 (2016).

32. J. Y. Yu, M. I. Kanai, E. Demir, G. S. X. E. Jefferis, B. J. Dickson, Cellular organization of the neural circuit that drives Drosophila courtship behavior. *Curr Biol* **20**, 1602–1614 (2010).

33. T. Liu, *et al.*, The receptor channel formed by ppk25, ppk29 and ppk23 can sense the Drosophila female pheromone 7,11-heptacosadiene. *Genes Brain Behav* **19**, e12529 (2020).

34. S. Kohatsu, M. Koganezawa, D. Yamamoto, Female contact activates male-specific interneurons that trigger stereotypic courtship behavior in Drosophila. *Neuron* **69**, 498–508 (2011).

562 35. H. K. Inagaki, K. M. Panse, D. J. Anderson, Independent, reciprocal neuromodulatory control of sweet and bitter
563 taste sensitivity during starvation in Drosophila. *Neuron* **84**, 806–820 (2014).

564 36. K. Sato, D. Yamamoto, Contact-Chemosensory Evolution Underlying Reproductive Isolation in Drosophila
565 Species. *Front Behav Neurosci* **14**, 597428 (2020).

566 37. T. Pizzari, T. R. Birkhead, Female feral fowl eject sperm of subdominant males. *Nature* **405**, 787–789 (2000).

567 38. R. H. Wagner, F. Helfenstein, E. Danchin, Female choice of young sperm in a genetically monogamous bird.
568 *Proc Biol Sci* **271 Suppl 4**, S134-137 (2004).

569 39. N. B. Davies, Polyandry, cloaca-pecking and sperm competition in dunnocks. *Nature* **302**, 334–336 (1983).

570 40. K. M. Lee, *et al.*, A neuronal pathway that controls sperm ejection and storage in female Drosophila. *Current*
571 *biology : CB* **25**, 790–797 (2015).

572 41. M. K. Manier, *et al.*, Resolving mechanisms of competitive fertilization success in Drosophila melanogaster.
573 *Science* **328**, 354–357 (2010).

574 42. C. Duménil, *et al.*, Pheromonal Cues Deposited by Mated Females Convey Social Information about Egg-Laying
575 Sites in Drosophila Melanogaster. *J Chem Ecol* **42**, 259–269 (2016).

576 43. G. Lee, J. C. Hall, J. H. Park, Doublesex gene expression in the central nervous system of Drosophila
577 melanogaster. *Journal of neurogenetics* **16**, 229–248 (2002).

578 44. C. Zhou, Y. Pan, C. C. Robinett, G. W. Meissner, B. S. Baker, Central brain neurons expressing doublesex
579 regulate female receptivity in Drosophila. *Neuron* **83**, 149–163 (2014).

580 45. D. J. Anderson, Circuit modules linking internal states and social behaviour in flies and mice. *Nat Rev Neurosci*
581 **17**, 692–704 (2016).

582 46. X. Jiang, Y. Pan, Neural Control of Action Selection Among Innate Behaviors. *Neurosci Bull* **38**, 1541–1558
583 (2022).

584 47. D.-H. Kim, Y.-H. Jang, M. Yun, K. M. Lee, Y.-J. Kim, Long-term neuropeptide modulation of the female sexual
585 drive via TRP channel in Drosophila melanogaster (Under Review on PNAS).

586 48. D. Deutsch, *et al.*, The neural basis for a persistent internal state in Drosophila females. *eLife* **9**, 1–74 (2020).

587 49. F. Wang, *et al.*, Neural circuitry linking mating and egg laying in Drosophila females. *Nature* **579**, 101–105
588 (2020).

589 50. C. E. Schretter, *et al.*, Cell types and neuronal circuitry underlying female aggression in Drosophila. *eLife* **9**, 1–
590 82 (2020).

591 51. C. Han, *et al.*, The doublesex gene regulates dimorphic sexual and aggressive behaviors in Drosophila.
592 *Proceedings of the National Academy of Sciences of the United States of America* **119** (2022).

593 52. H. Chiu, *et al.*, Cell type-specific contributions to a persistent aggressive internal state in female Drosophila.
594 2023.06.07.543722 (2023).

595 53. M. Laturney, J.-C. Billeter, Drosophila melanogaster females restore their attractiveness after mating by
596 removing male anti-aphrodisiac pheromones. *Nat Commun* **7**, 12322 (2016).

597 54. W. van der Goes van Naters, J. R. Carlson, Receptors and neurons for fly odors in Drosophila. *Curr Biol* **17**,
598 606–612 (2007).

599 55. A. Couto, M. Alenius, B. J. Dickson, Molecular, Anatomical, and Functional Organization of the Drosophila
600 Olfactory System. *Current Biology* **15**, 1535–1547 (2005).

601 56. C.-C. Lin, C. J. Potter, Re-Classification of Drosophila melanogaster Trichoid and Intermediate Sensilla Using
602 Fluorescence-Guided Single Sensillum Recording. *PLoS One* **10**, e0139675 (2015).

603 57. S. T. Sweeney, K. Broadie, J. Keane, H. Niemann, C. J. O'Kane, Targeted expression of tetanus toxin light chain
604 in Drosophila specifically eliminates synaptic transmission and causes behavioral defects. *Neuron* **14**, 341–351
605 (1995).

606 58. F. N. Hamada, *et al.*, An internal thermal sensor controlling temperature preference in Drosophila. *Nature* **454**,
607 217–220 (2008).

608 59. J.-C. Billeter, J. Atallah, J. J. Krupp, J. G. Millar, J. D. Levine, Specialized cells tag sexual and species identity
609 in Drosophila melanogaster. *Nature* **461**, 987–991 (2009).

610 60. Z. Wang, *et al.*, Desiccation resistance differences in Drosophila species can be largely explained by variations
611 in cuticular hydrocarbons. *Elife* **11**, e80859 (2022).

612 61. D. Scott, R. C. Richmond, A genetic analysis of male-predominant pheromones in Drosophila melanogaster.
613 *Genetics* **119**, 639–646 (1988).

614 62. R. Thistle, P. Cameron, A. Ghorayshi, L. Dennison, K. Scott, Contact chemoreceptors mediate male-male
615 repulsion and male-female attraction during Drosophila courtship. *Cell* **149**, 1140–1151 (2012).

616 63. V. Vijayan, R. Thistle, T. Liu, E. Starostina, C. W. Pikielny, Drosophila pheromone-sensing neurons expressing
617 the ppk25 ion channel subunit stimulate male courtship and female receptivity. *PLoS Genet* **10**, e1004238 (2014).

618 64. B. Lu, A. LaMora, Y. Sun, M. J. Welsh, Y. Ben-Shahar, ppk23-Dependent chemosensory functions contribute to
619 courtship behavior in Drosophila melanogaster. *PLoS Genet* **8**, e1002587 (2012).

620 65. G. A. Parker, Sperm Competition and Its Evolutionary Consequences in the Insects. *Biological Reviews* **45**, 525–
621 567 (1970).

622 66. A. F. Dixson, *Primate Sexuality: Comparative Studies of the Prosimians, Monkeys, Apes, and Human Beings*
623 (Oxford University Press, 1998).

624 67. M. R. Schneider, R. Mangels, M. D. Dean, The molecular basis and reproductive function(s) of copulatory plugs.
625 *Mol Reprod Dev* **83**, 755–767 (2016).

626 68. R. Dean, S. Nakagawa, T. Pizzari, The risk and intensity of sperm ejection in female birds. *Am Nat* **178**, 343–
627 354 (2011).

628 69. G. Bontonou, B. Denis, C. Wicker-Thomas, Interaction between temperature and male pheromone in sexual
629 isolation in Drosophila melanogaster. *J Evol Biol* **26**, 2008–2020 (2013).

630 70. M. Werthebach, *et al.*, Control of Drosophila Growth and Survival by the Lipid Droplet-Associated Protein
631 CG9186/Sturkopf. *Cell Rep* **26**, 3726-3740.e7 (2019).

632 71. C. Everaerts, J.-P. Farine, M. Cobb, J.-F. Ferveur, Drosophila cuticular hydrocarbons revisited: mating status
633 alters cuticular profiles. *PLoS One* **5**, e9607 (2010).

634 72. L. K. Scheffer, *et al.*, A connectome and analysis of the adult Drosophila central brain. *eLife* **9**, e57443 (2020).

635 73. Y. J. Kim, *et al.*, Galactoside in the male ejaculate evaluated as a nuptial gift by the female nutrient sensing
636 neurons (2023) https:/doi.org/10.21203/rs.3.rs-2137467/v1 (October 18, 2023).

637 74. C.-C. Lin, K. A. Prokop-Prigge, G. Preti, C. J. Potter, Food odors trigger Drosophila males to deposit a
638 pheromone that guides aggregation and female oviposition decisions. *Elife* **4**, e08688 (2015).

639 75. T. A. Verschut, *et al.*, Aggregation pheromones have a non-linear effect on oviposition behavior in Drosophila
640 melanogaster. *Nat Commun* **14**, 1544 (2023).

641 76. A. K. Tanenhaus, J. Zhang, J. C. P. Yin, In vivo circadian oscillation of dCREB2 and NF-κB activity in the
642 Drosophila nervous system. *PloS one* **7** (2012).

643 77. J. J. Bussell, N. Yapici, S. X. Zhang, B. J. Dickson, L. B. Vosshall, Abdominal-B neurons control Drosophila
644 virgin female receptivity. *Curr Biol* **24**, 1584–1595 (2014).

645 78. N. C. Klapoetke, *et al.*, Independent optical excitation of distinct neural populations. *Nature methods* **11**, 338–
646 346 (2014).

647 79. F. Mohammad, *et al.*, Optogenetic inhibition of behavior with anion channelrhodopsins. *Nat Methods* **14**, 271–
648 274 (2017).

649 80. S. Schröder-Lang, *et al.*, Fast manipulation of cellular cAMP level by light in vivo. *Nat Methods* **4**, 39–42 (2007).

650 81. K. E. Yu, D.-H. Kim, Y.-I. Kim, W. D. Jones, J. E. Lee, Mass Spectrometry-Based Screening Platform Reveals
651 Orco Interactome in Drosophila melanogaster. *Mol Cells* **41**, 150–159 (2018).

652 82. N. Yapici, Y. J. Kim, C. Ribeiro, B. J. Dickson, A receptor that mediates the post-mating switch in Drosophila
653 reproductive behaviour. *Nature* **451**, 33–37 (2008).

654 83. S. Kohatsu, D. Yamamoto, Visually induced initiation of Drosophila innate courtship-like following pursuit is
655 mediated by central excitatory state. *Nat Commun* **6**, 6457 (2015).

656 84. J. A. Bogovic, *et al.*, An unbiased template of the Drosophila brain and ventral nerve cord. *PLOS ONE* **15**,
657 e0236495 (2020).

658 85. H. Otsuna, M. Ito, T. Kawase, Color depth MIP mask search: a new tool to expedite Split-GAL4 creation. 318006
659 (2018).

660 86. J. Clements, *et al.*, NeuronBridge: an intuitive web application for neuronal morphology search across large data
661 sets. 2022.07.20.500311 (2022).

662
663

Figures and Tables

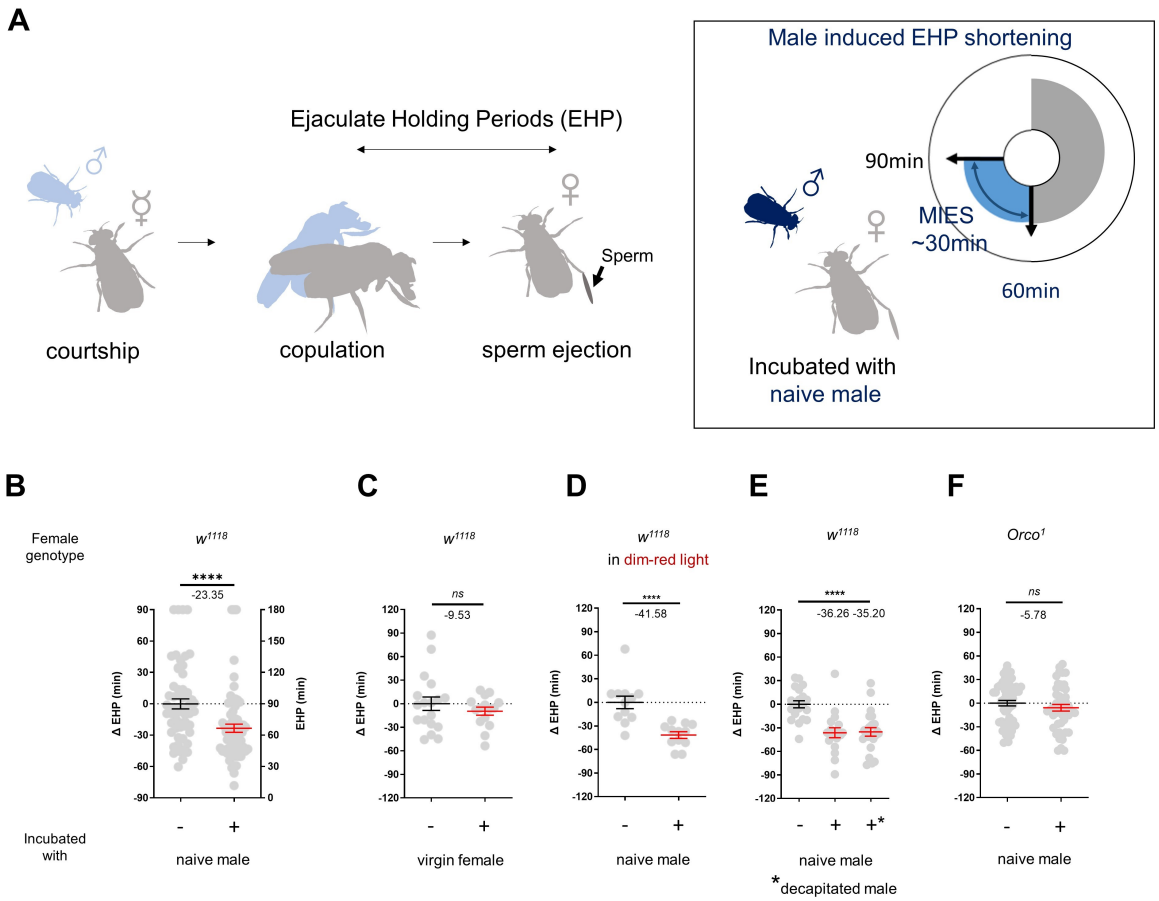

Fig. 1. The presence of males shortens the ejaculate holding period (EHP) in females through olfactory or gustatory sensation

A, Schematic of the experimental procedure to measure male-induced EHP shortening (MIES). A female mates with a wild-type *Canton-S* (*CS*) male. Immediately after mating, the female is incubated with a naïve male. Typically, females kept alone exhibit an EHP of approximately 90 min, whereas females incubated with a naïve male exhibit an EHP of approximately 60 min. In this study, we refer to this phenomenon as male-induced EHP shortening (MIES).

B-F, Ejaculation holding period (EHP) or ΔEHP of the females of the indicated genotypes, incubated under the indicated conditions after mating. Normalized EHP (ΔEHP) is calculated by subtracting the mean of reference EHP of females kept alone after mating (leftmost column) from the EHP of females incubated with other flies.

Mann-Whitney Test (n.s. $p > 0.05$; ****$p < 0.0001$). Gray circles indicate the EHP or ΔEHP of individual females, and the mean ± SEM of data is presented. Numbers below the horizontal bar represent the mean of EHP differences between treatments.

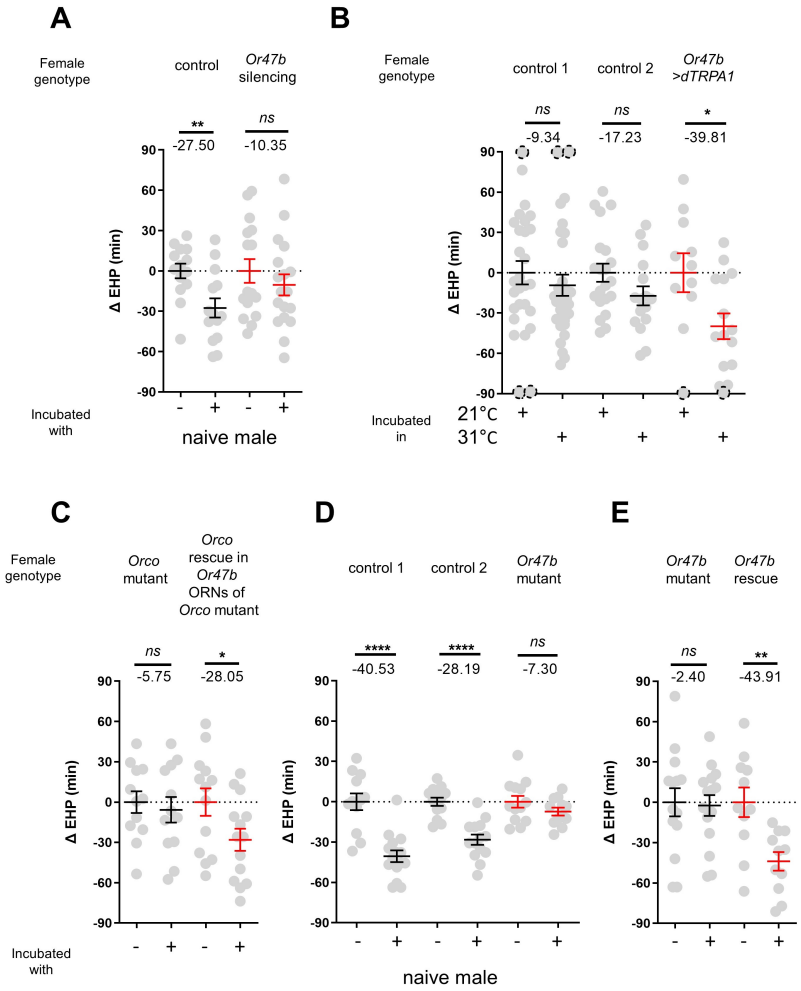

Fig. 2. Or47b and Or47b-positive ORNs are required for MIES

A, C-E, ΔEHP of females of the indicated genotypes, incubated with or without naive males. Female genotypes are as follows from left to right: (A) control (*Or47b>TNT^{inactive}*), *Or47b* ORN silencing (*Or47b>TNT^{active}*); (C) *Orco* mutant (*Orco^{1}/Orco^{1}*), *Orco* rescue in *Or47b* ORNs of *Orco* mutant (*Orco^{1}/Orco^{1}*; *Or47b>Orco*); (D) control 1 (*Or47b^{2}/+*), control 2 (*Or47b^{3}/+*), *Or47b* mutant (*Or47b^{2}/Or47b^{3}*); (E) *Or47b* mutant *(Or47b^{2}/Or47b^{2}*), *Or47b* rescue (*Or47b>Or47b; Or47b^{2}/Or47b^{2}*).

B, Thermal activation of *Or47b*-positive ORNs shortens EHP in the absence of naive males. ΔEHP is calculated by subtracting the mean of reference EHP of females incubated at 21°C control conditions from the EHP of individual females. Female genotypes are as follows from left to right: control 1 (*Or47b-Gal4/+),* control 2 (*UAS-dTRPA1/+), Or47b>dTRPA1 (Or47b-Gal4/UAS-dTRPA1*).

Mann-Whitney Test (n.s. $p > 0.05$; *$p < 0.05$; **$p < 0.01$; ****$p < 0.0001$). Gray circles indicate the ΔEHP of individual females, and the mean ± SEM of data is presented. Gray circles with dashed borders indicate ΔEHP values beyond the axis limits (>90 or <-90 min). Numbers below the horizontal bar represent the mean of EHP differences between treatments.

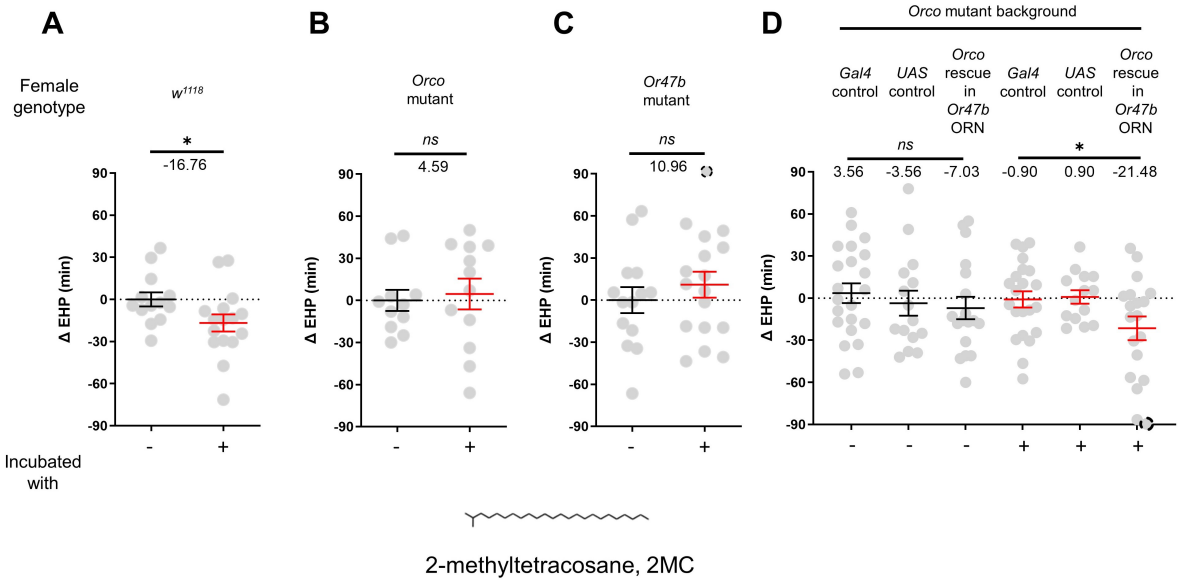

Fig. 3. 2-methyltetracosane (2MC) can induce EHP shortening through Or47b A-D, Δ EHP of mated females of the indicated genotypes, incubated in solvent vehicle or 2MC. Mated females were incubated with a piece of filter paper perfumed with vehicle (-) or 750 ng 2MC (+). Female genotypes are as follow: (A) *w*^{1118}, (B) *Orco* mutant (*Orco*^{1}/*Orco*^{1}), (C) *Or47b* mutant (*Or47b*^{2}/*Or47b*^{2}), (D) *Gal4* control (*Or47b-Gal4/+*; *Orco*^{1}/*Orco*^{1}), *UAS* control (*UAS-Orco/+*; *Orco*^{1}/*Orco*^{1}), *Orco* rescue in *Or47b* ORN (*Orco*^{1}/*Orco*^{1}; *Or47b-Gal4/UAS-Orco*).
A-C, Mann-Whitney Test (n.s. $p > 0.05$; *$p < 0.05$), D, One-way analysis of variance (ANOVA) test (n.s. $p > 0.05$; *$p < 0.05$). Gray circles indicate the ΔEHP of individual females and the mean ± SEM of data is presented. Normalized EHP (ΔEHP) is calculated by subtracting the mean of reference EHP of females incubated with vehicle (A-C) or mean of *Gal4* control and *UAS* control female incubated with vehicle (D) after mating from the EHP of females incubated with chemical perfumed paper. Gray circles with dashed borders indicate ΔEHP values beyond the axis limits (>90 or <-90 min). Numbers below the horizontal bar represent the mean of EHP differences between treatments.

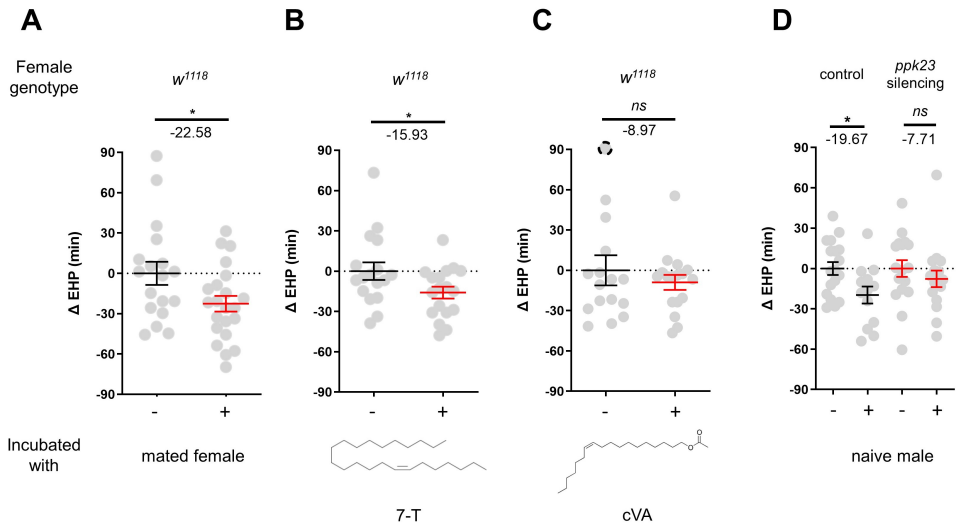

Fig. 4. 7-Tricosene present in mated females or naive males shorten EHP via *ppk23* neurons
A-D, ΔEHP of females of the indicated genotypes, incubated with mated females (A), a piece of filter paper perfumed with 150 ng 7-T (B) or 200 ng cVA (C), or naive males (D) immediately after mating. Female genotypes are: (A-C) w^{1118}, (D) control (*ppk23-Gal4/UAS-TNT*^{inactive}), *ppk23* silencing (*ppk23-Gal4/UAS-TNT*^{active}).
Unpaired *t*-Test (n.s. $p > 0.05$; * $p < 0.05$). Gray circles indicate the ΔEHP of individual females, and the mean ± SEM of data is presented. Gray circles with dashed borders indicate ΔEHP values beyond the axis limits (>90 or <-90 min). Numbers below the horizontal bar represent the mean of EHP differences between treatments.

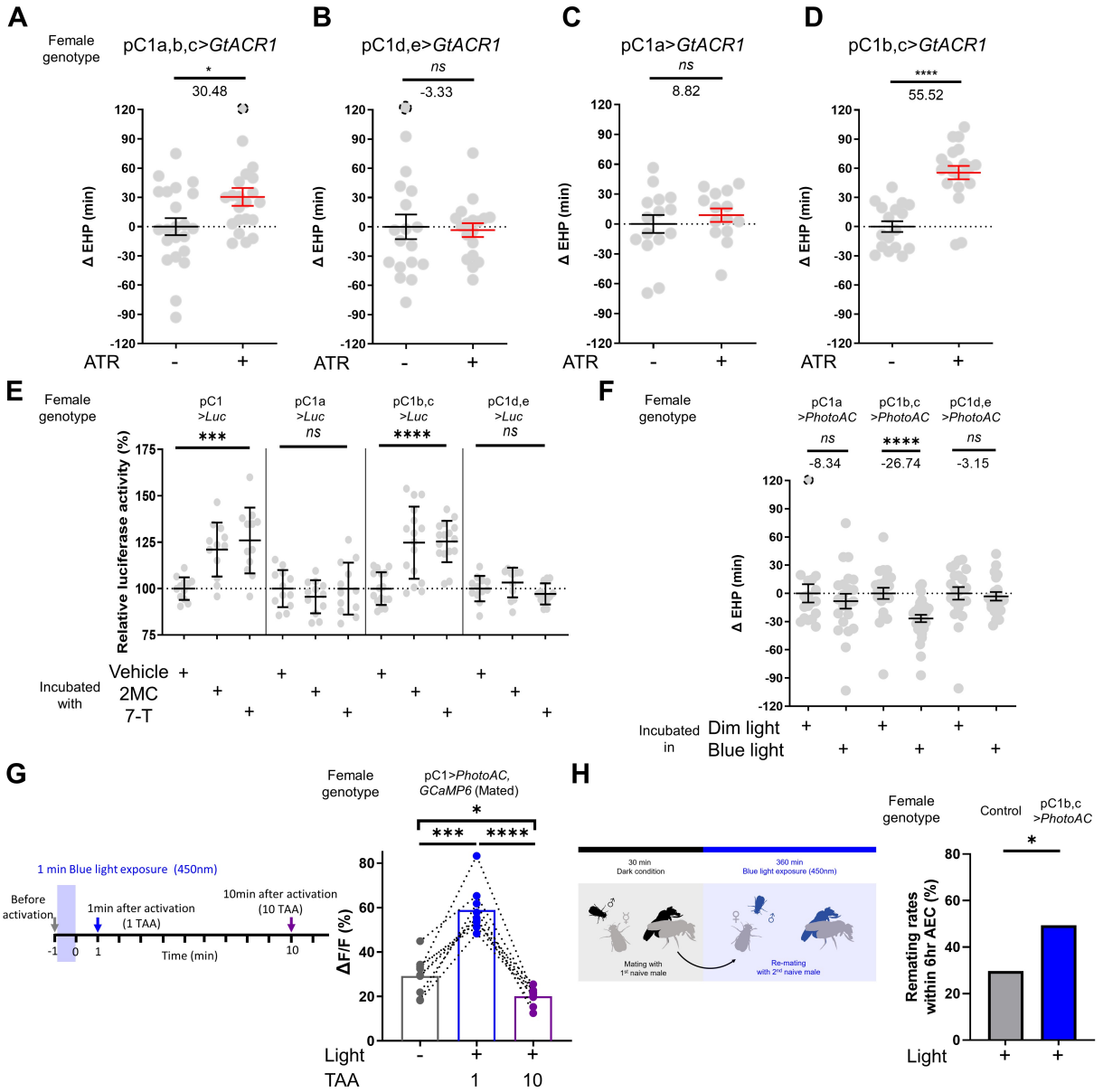

Fig. 5. pC1 neuron subset comprising pC1b and c subtypes regulates EHP in response to 2MC and 7-T, both of which upregulate cAMP activity and excitability of pC1 neurons

A-D, Optogenetic silencing of a pC1 neuron subset comprising pC1b and c subtypes increases EHP. Females of the indicated genotypes were cultured on food with or without all-*trans*-retinal (ATR). ΔEHP is calculated by subtracting the mean of reference EHP of females cultured in control ATR- food from the EHP of individual test females. Female genotypes are: (A) pC1a,b,c>*GtACR1* (*pC1-S-Gal4/UAS-GtACR1*), (B) pC1d,e>*GtACR1* (*pC1-A-Gal4/UAS-GtACR1*), (C) pC1a>*GtACR1* (*pC1a-split-Gal4 /UAS-GtACR1*), and (D) pC1b,c>*GtACR1* (*Dh44-pC1-Gal4/UAS-GtACR1*). Gray circles indicate the ΔEHP of individual females, and the mean ± SEM of data is presented. Gray circles with dashed borders indicate ΔEHP values beyond the axis limits (>120 min). Mann-Whitney Test (n.s. $p > 0.05$; *$p < 0.05$; ****$p < 0.0001$). Numbers below the horizontal bar represent the mean of EHP differences between treatments.

E, Relative *CRE-Luciferase* reporter activity of pC1 neurons in mated females of the indicated genotypes, incubated with a piece of filter paper perfumed with solvent vehicle control or the indicated odorants. To calculate the relative luciferase activity, we set the average luminescence unit values of female incubated with the vehicle to 100%. One-way ANOVA test (n.s. $p > 0.05$; ***$p < 0.001$; ****$p < 0.0001$). Gray circles indicate the relative luciferase activity (%) of individual females, and the mean ± SEM of data is presented.

F, Optogenetic production of cAMP in the pC1 b and c neurons shortens EHP, whereas the same treatment in pC1a or pC1d and e neurons does not. ΔEHP is calculated by subtracting the mean of reference EHP of females incubated in the control illumination (Dim light), which does not activate a

743 photoactivatable adenylate cyclase (PhotoAC), from the EHP of individual test females. Mann-Whitney
744 Test (n.s. $p > 0.05$, ****$p < 0.0001$).
745 **G**, Optogenetic production of cAMP increases excitability of pC1 neurons transiently. Left, schematic of the
746 experimental procedure. Right, peak ΔF/F in the LPC projections of pC1 neurons from freshly mated
747 females in response to the pheromone cVA, before and after photoactivation of PhotoAC expressed in
748 pC1 neurons. Calcium response was measured at specific time points: after 1 minute (Blue dots and box,
749 1 TAA = 1 Time After Activation) or 10 minutes (Purple dots and box, 10 TAA) after activation. Repeated
750 measures (RM) one-way ANOVA test with the Geisser-Greenhouse correction followed by Tukey's
751 multiple comparisons test (*$p < 0.05$; ***$p < 0.001$; ****$p < 0.0001$).
752 **H**, Left, schematic of the experimental procedure. Right, re-mating rate of females during optogenetic
753 cAMP production in pC1b and c, scored as the percentage of females that copulate with naive male within
754 6 h after end of first mating. Female genotypes are control (+/*UAS-PhotoAC*), pC1b,c>*UAS-PhotoAC*
755 (*Dh44-pC1-Gal4/UAS-PhotoAC*). Chi-square test (*$p < 0.05$).
756